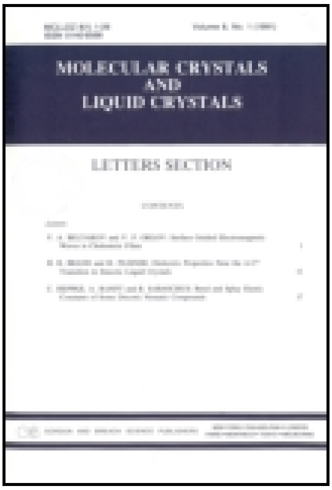

Molecular Crystals and Liquid Crystals
Publication details, including instructions for authors and subscription information:
http://www.tandfonline.com/loi/gmcl20

Inkjet Printed Poly(3-hexylthiophene) Thin-Film Transistors: Effect of Self-Assembled Monolayer

Mengjie Chen[ab], Rui Peng[ab], Xianfeng Xiong[a], Shiqin Chen[ab], Guobing Zhang[ab], Hongbo Lu[ab], Xianghua Wang[a] & Longzhen Qiu[ab]

[a] Key Lab of Special Display Technology, Ministry of Education, National Engineering Lab of Special Display Technology, National Key Lab of Advanced Display Technology, Academy of Opto-Electronic Technology, Hefei University of Technology, Hefei, China

[b] Key Laboratory of Advanced Functional Materials and Devices, School of Chemical Engineering, Hefei University of Technology, Hefei, China

Published online: 27 May 2014.

To cite this article: Mengjie Chen, Rui Peng, Xianfeng Xiong, Shiqin Chen, Guobing Zhang, Hongbo Lu, Xianghua Wang & Longzhen Qiu (2014) Inkjet Printed Poly(3-hexylthiophene) Thin-Film Transistors: Effect of Self-Assembled Monolayer, Molecular Crystals and Liquid Crystals, 593:1, 201-213, DOI: 10.1080/15421406.2013.873596

To link to this article: http://dx.doi.org/10.1080/15421406.2013.873596

Mol. Cryst. Liq. Cryst., Vol. 593: pp. 201–213, 2014

ISSN: 1542-1406 print/1563-5287 online
DOI: 10.1080/15421406.2013.873596

Inkjet Printed Poly(3-hexylthiophene) Thin-Film Transistors: Effect of Self-Assembled Monolayer

MENGJIE CHEN,[1,2] RUI PENG,[1,2] XIANFENG XIONG,[1]
SHIQIN CHEN,[1,2] GUOBING ZHANG,[1,2] HONGBO LU,[1,2]
XIANGHUA WANG,[1,*] AND LONGZHEN QIU[1,2,*]

[1]Key Lab of Special Display Technology, Ministry of Education, National Engineering Lab of Special Display Technology, National Key Lab of Advanced Display Technology, Academy of Opto-Electronic Technology, Hefei University of Technology, Hefei, China
[2]Key Laboratory of Advanced Functional Materials and Devices, School of Chemical Engineering, Hefei University of Technology, Hefei, China

Organic thin film transistors (OTFTs) with bottom gate and top contact structure had been prepared by inkjet printing. It is found that the surface properties of the substrates have a great influence on the morphology of the inkjet printed droplet and film. An appropriate surface was vital to form a uniform semiconducting film by inkjet printing and also strongly improved the electric characteristics. When a bare SiO_2 layer was applied, the best field-effect mobility of inkjet printed OTFT devices was only 2.37×10^{-3} $cm^2V^{-1}s^{-1}$, with an on/off current ratio of 10^2. When the PETS treatment or the PTS treatment was applied on the SiO_2 dielectric layer, the field-effect performances were substantially improved and the best field-effect mobility was enhanced to 8.07×10^{-3} $cm^{-2}V^{-1}s^{-1}$ and 7.95×10^{-3} $cm^{-2}V^{-1}s^{-1}$, respectively and with an on/off current ratio of 10^3.

Keywords Inkjet print; organic thin film transistor; poly(3-hexyl)thiophene; self-assembled monolayers

Introduction

Over the past decades, there was a fast progress in the field of organic thin-film transistors (OTFTs) [1 , 2]. The interest arises from the unique advantages of organic semiconductors including light weight, low-cost, good compatibility with flexible substrates, and great opportunities in structural modifications [3–5]. In particular, the conjugated polymer semiconductors enable process via high-throughput printing process instead of traditional silicon technologies, which offers an appealing approach to creating ultra low-cost, large-area printed electronics [6–8]. There are a large number of reports on the preparation of OTFTs

*Address correspondence to Xianghua Wang and Longzhen Qiu, Key Lab of Special Display Technology, Ministry of Education, National Engineering Lab of Special Display Technology, National Key Lab of Advanced Display Technology, Academy of Opto-Electronic Technology, Hefei University of Technology, Hefei 230009, China, and Key Laboratory of Advanced Functional Materials and Devices, School of Chemical Engineering, Hefei University of Technology, Hefei 230009, China. E-mail: xhwang@hfut.edu.cn for Xianghua Wang, and lzhqiu@hfut.edu.cn for Longzhen Qiu.

using established printing technologies such as micro-contact printing [9], screen printing [6], gravure printing [10], nanotransfer [11], or inkjet printing [12–14]. Among them, inkjet printing is very promising because it is a drop-on-demand digital lithographic approach without using other lithography process and physical masks which leads to cost-savings and pattern with ease [15–19]. However, the inkjet printing of organic semiconductor films with uniform morphology and desired crystalline microstructures is challenging for the achievement of high-performance printed devices [20–23].

It has been reported that the semiconductor/dielectric interface plays a key role in the improvement of OTFT performance because the surface characteristics of the dielectric can determine the growth of the semiconductor in the first few monolayers which is the main transport channel of carriers [24 , 25]. In order to control the dielectric surface properties for favorable mesoscale/nanoscale ordering of organic semiconductors, one of the most practical methods is to insert an interface buffer layer such as a self-assembled monolayer (SAM) or a thin polymeric layer between the gate dielectric and the semiconductor due to the easy fabrication of such layers with nanoscale thickness [26 , 27]. For solution-processed OTFTs, organosilanes SAMs are preferential due to their insolubility in most organic solvents because they are anchored on the surface by chemical bonds. The performance of solution-processed OTFTs can be efficiently improved by treating the dielectric surface with alkylsilane such as octadecyltrichlorosilane and octyltrichlorosilane (OTS) because the presence of a SAM layer can reduce the number of charge trapping states at the interface by covering silanol groups and ionic impurities of SiO_2 [28–30]. Furthermore, the treatment of dielectric surface with alkylsilane makes the surface hydrophobic and smooth, which induced order molecular orientation of semiconductors.

However, in the case of inkjet printing of organic semiconductors, the wetting and evaporation behaviors of inkjet-deposited droplets on the substrate surface should also be concerned [31]. If the surface wetting for inkjet printing is inadequate to pin the contact line of the droplet on the surface, the contact diameter tends to recede continuously during solvent evaporation and the solutes will be concentrated at the center of the droplet, which hinters the formation of uniform films and reduces the printing accuracy [32]. Therefore, a surface with suitable wettability is very important for the fabrication of high-performance organic transistors via inkjet printing.

In this work, the effect of surface property of semiconductor-insulator interface on inkjet printed organic semiconductor OTFT devices of poly(3-hexylthiophene) (P3HT) was investigated. Three kinds of SAMs have been introduced onto the SiO_2 gate dielectrics to alter the surface energy. We study the impact of surface property on the morphology and microstructures of inkjet-printed single droplets and films. We also examine the dependence of the field-effect electrical performance of inkjet printed P3HT films on surface treatment with different kinds of SAM layer.

Experimental

Materials

Regioregular P3HT (Mw $\sim$ 50 kg mol^{-1}) was obtained from the Rieke Metals Incorporation. Phenyltrichlorosilane (PTS), phenethyltricholosilane (PETS) were purchased from J&K Chemical. OTS, 1, 2, 4-Trichlorobenzene (TCB) were purchased from Aldrich Chemical Co. All materials were used as received without further purification and their chemical structures were displayed in Fig. 1, respectively.

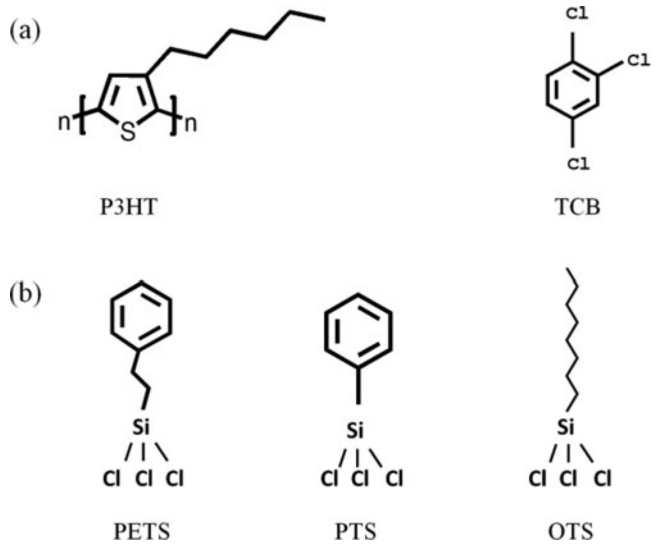

Figure 1. Chemical structure of (a) poly(3-hexylthiophene) (P3HT), (b) 1,2,4-trichlorobenzene (TCB), (c) phenethyltricholosilane (PETS), (d) phenyltrichlorosilane (PTS), and (e) octyltrichlorosilane (OTS).

Preparation of Self-Assembled Monolayer

The heavily doped *n*-type Si wafer capped with a 300-nm-thick thermally grown oxide layer is employed as the substrate for inkjet printing of the organic semiconductor. For OTFT device fabrication, the *n*-type Si and the oxide layer is used as the gate electrode and gate dielectric respectively. The wafer was firstly cleaned with acetone, ethanol, and distilled water in sequence followed by nitrogen blow-off. Prior to the surface treatment, the wafer was cleaned in piranha solution (70 vol% H_2SO_4 + 30 vol% H_2O_2) for 40 min at 90°C and rinsed with copious amounts of distilled water.

Vacuum-dried reaction flasks were filled with anhydrous toluene and the cleaned silicon wafers or cover glasses under argon protection. Solutions of the alkylsilanes (10 mM) were then added to the flask to be self-assembled on the wafers for 1 hr under argon atmosphere. The treated wafers were rinsed with toluene and ethanol several times and then baked in an oven at 120°C for 30 min. After baking, the samples were unltrasonic cleaned in toluene, then rinsed thoroughly with ethanol, and finally vacuum driedying for inkjet printing.

Inkjet Printing Process

Inkjet printing was performed with a Dimatix DMP3000 printer in a 25°C air-conditioned ambient environment with the relative humidity controlled at 50%. P3HT was dissolved in TCB at a concentration of 6.5 mg mL^{-1} and injected into the cartridge equipped with 16 squarish nozzles through a 0.45 μm tetrafluoroethylene filter. Each nozzle of the jetting module, 21 μm in diameter, normally produces a 10 pL droplet in each ejection. The jetting frequency was fixed at 1 kHz in all printing process, and the jetting velocity was adjusted around 2.5 m/s. We have optimized the jetting parameters in order to make stable droplets with good repeatability and to remove satellite drops before printing onto the substrate.

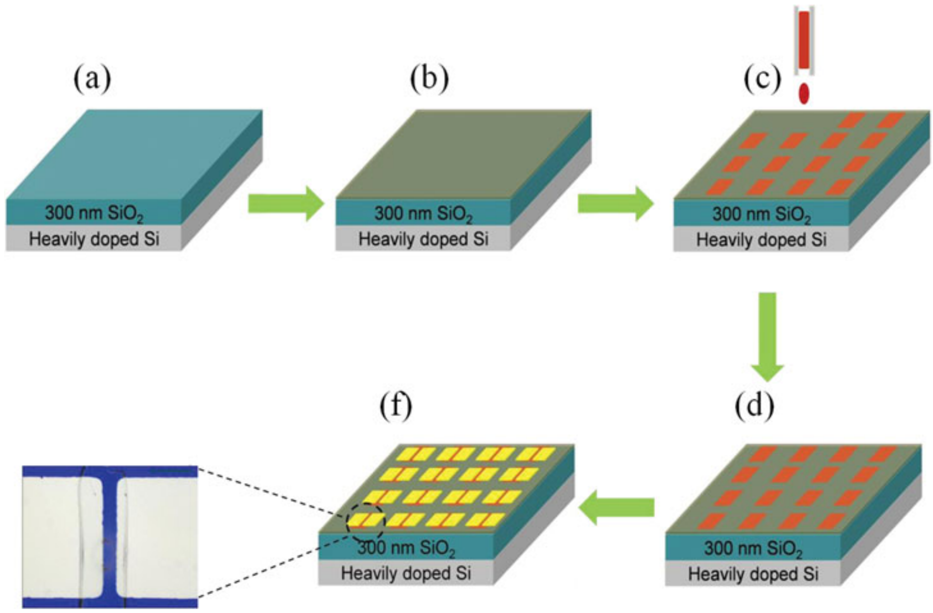

Figure 2. Schematic illustration of the fabrication of inkjet printed OTFTs on the substrates with different treatments.

Preparation of OTFT Devices

Figure 2 schematically describes the fabrication of OTFTs with different SAM-treated SiO_2 layer in this work. Firstly, a heavily doped, *n*-type Si wafer with 300 nm thermal oxide (capacitance = 10.8 nFcm^{-2}) was carefully cleaned and grown with a SAM to modify the hydrophilic oxide surface. Then the P3HT films were prepared by inkjet printing and then vacuum annealed at 120°C for 20 min to remove the residual solvent. A 60-nm-thick Au layer was prepared by thermal evaporation and patterned through shadow masks (channel length = 80 μm, channel width = 800 μm) on the film to form the source-drain electrodes.

Measurements

The surface property of the prepared SAMs was determined by measuring the contact angle with an OCA15 video-based automatic contact angle measuring instrument from Data Physics. The surface energy of SAMs was calculated from the contact angle of distilled water and diiodomethane measured at a room temperature of 25°C. The electrical characteristics of the OTFT devices were measured in the accumulation mode using Keithley 4200 units under ambient conditions. The film morphology was characterized by a fiducial camera, an optical substrate inspection system of the inkjet printer and the atomic force microscope (AFM) (Digital Instruments Multimode) operated in tapping mode.

Result and Discussion

The SAM can chemically modify the surface property of the SiO_2 dielectric layer since the silane can react with –OH groups on the SiO_2 surface and form a SAM, as shown in Fig. 3.

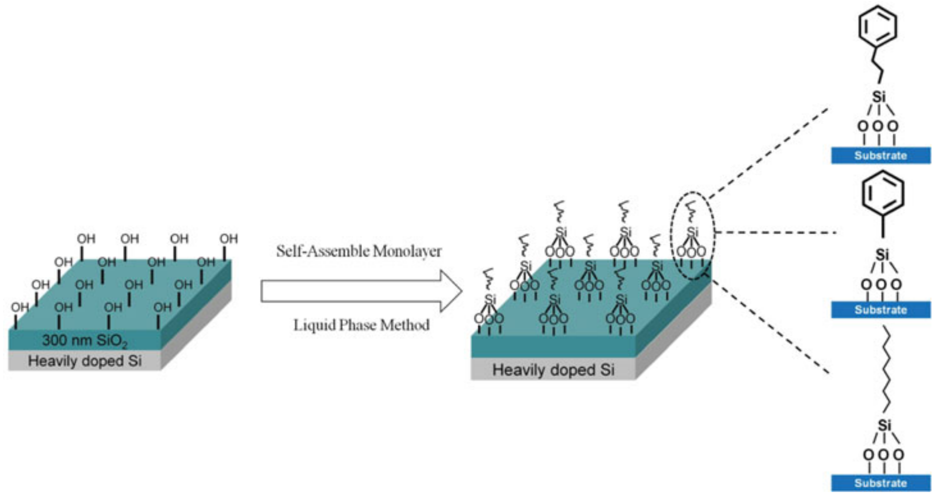

Figure 3. Schematic diagram showing the forming process of self-assemble monolayer.

Change in surface property of the SAM-treated SiO_2 layer was confirmed by contact angle analysis as shown in Fig. 4. It was clearly observed that self-assembled mono layer made the surface of SiO_2 layer more hydrophobic.

The surface energy (Fig. 5) of the substrates including the dispersion component $\gamma_s{}^d$ and the polar component $\gamma_s{}^p$ were evaluated from contact angle measurements using distilled water and diiodomethane (CH_2I_2) as test liquids; their values were calculated according to the geometric mean method based on the equation:

$$(1 + cos\theta_t)\gamma_t = 2\{(\gamma_t^d \gamma_s^d)^{1/2} + (\gamma_t^p \gamma_s^p)^{1/2}\},$$

where θ is the contact angle of the test liquid on a solid surface, and γ_t and γ_s are the surface energies of the test liquid and solid surface, respectively.

Due to the high density of hydroxyl group on the surface, the wafer cleaned in the piranha solution showed a high surface energy up to 68.29 mJm^{-2}. However, a substrate with

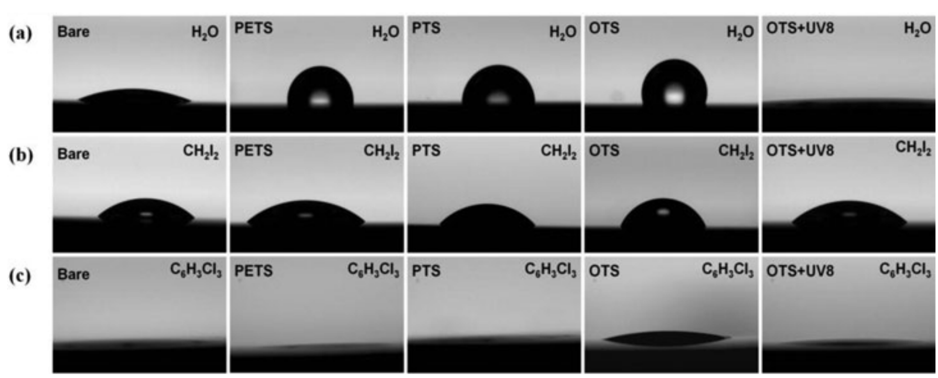

Figure 4. Contact angles of different test liquid on the substrates with different treatments: (a) water, (b) diiodomethane, and (c) 1, 2, 4-trichlorobenzene.

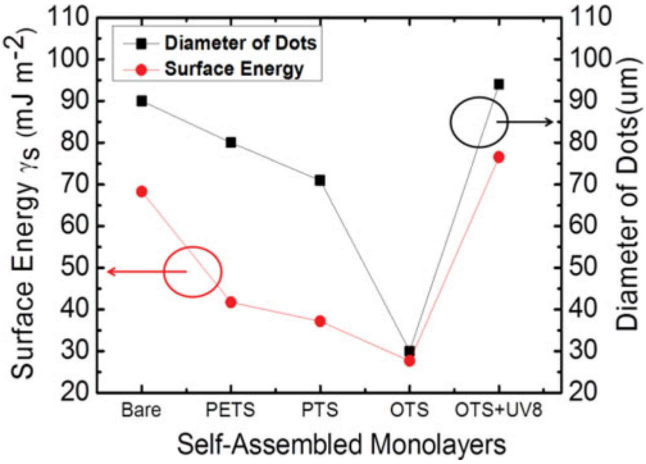

Figure 5. Surface energy and droplet diameter on the surfaces with different treatments.

such a high surface energy was instable in an ambient air environment since contaminants in the air adhered onto the surface rapidly. Organosilanes can be effectively connected to the hydroxylated substrates via forming Si−O−Si bonds which resulted in the replacement of the natural hydroxyl group on the SiO_2 substrate with hydrophobic group. The treatment of hydroxylated wafer with PETS, PTS, and OTS considerably reduced the surface energy from 68.29 to 41.71, 37.16, and 27.69 mJm^{-2}, respectively (Fig. 5). In addition, the surface property after silane treatment became more stable which was beneficial to prolonged and reliable inkjet printing in the air ambient.

A solution of P3HT dissolved in trichlorobenzene (6.5 mg mL^{-1}) was inkjet-printed on the surface-modified dielectrics. The morphologies of inkjet-printed single droplets and films of P3HT deposited on various SAMs are shown in Fig. 6. The diameters of the single droplets on bare surface were about 90 μm and were much larger than the dimension of a spherical 10 pL flying droplet, suggesting high wettability of the ink solution on bare substrates. In the case of PETS-, PTS-, or OTS-treated surfaces, the surface energy is lower compared to bare surface and the droplet diameter decreases monotonously to 80, 71, and 30 μm, respectively, with the reduction of the surface energy as plotted in

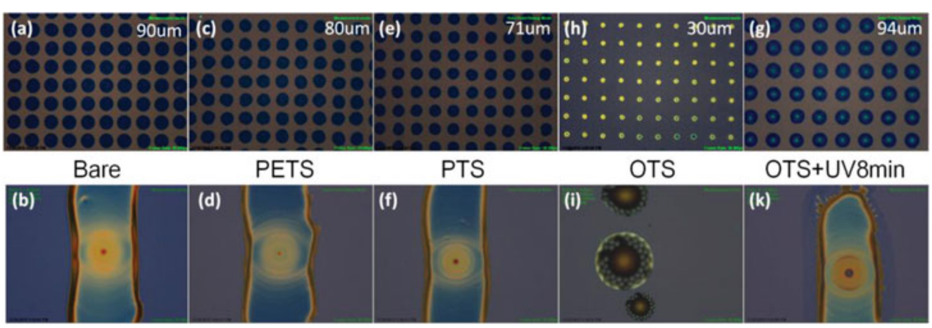

Figure 6. The morphology of the inkjet printed droplets and films on the substrates with different treatments.

Fig. 5. P3HT films in the geometry of a 0.24 mm × 1.20 mm rectangle were also printed at 20 μm drop spacing on the substrates with different surface treatment using three adjacent nozzles. The jetting velocity of the flying droplets is 2.5 m s^{-1}. Images of the printed films were immediately taken with a fiducial camera, an optical substrate inspection system of the inkjet printer, as shown in Fig. 6 (b, d, f, and i). It can be observed that a continuous film can be obtained on the bare SiO_2 wafer (Fig. 6b) the PETS-treated (Fig. 6d) and the PTS-treated (Fig. 6f) SiO_2 wafer. Moreover, the printed films based on the PETS-treated and PTS-treated wafer were more transparent and uniform than those prepared on bare SiO_2. However, in the case of OTS-treated wafer, the P3HT film is incontinuous (Fig. 6i).

There are two basic evaporation modes for a droplet on a substrate. One is the constant diameter mode in which the contact line of the droplet is pinned immediately after deposition and remained constant until complete drying, the other is the constant contact angle mode in which the contact angle of the droplet on the surface remains constant with decreasing contact diameter as the evaporation proceeds. As the surface energies of the bare, PETS-, and PTS-treated silicon wafers are higher than or comparable to the surface tension of trichorobezene (i.e., 39.9 dyne/cm), the ink droplets wet well on these substrates, and thus dry in the constant contact diameter mode. In contrast, the OTS-treated substrate has a very low surface energy and is nonwettable to the solvent, which can also be confirmed by the contact angle measurements using the solvent of TCB as shown in Fig. 4c. The contact angle measured on the PETS-, PTS-, or OTS + UV8min-treated wafer was very close to 0°, while it was about 13° on the OTS-treated wafer. The contact line recedes without pinning during the evaporation, and as a result the single droplet shrinks to small size and no continuous film forms the OTS-treated wafer. The hydrophobic surface with SAM-modifier can reversely become hydrophilic by treating the substrates with UV-ozone. While a UV-ozone clean was applied for 8 min, the isolating dots printed on the substrate were dramatically enlarged from 30 μm (Fig. 6h) to 94 μm (Fig. 6g) and a continuous film can be printed as shown in Fig. 6k.

AFM was used to examine the surface topography of the films. Fig. 7 shows AFM height and phase images of the P3HT thin films inkjet printed on four different substrates.

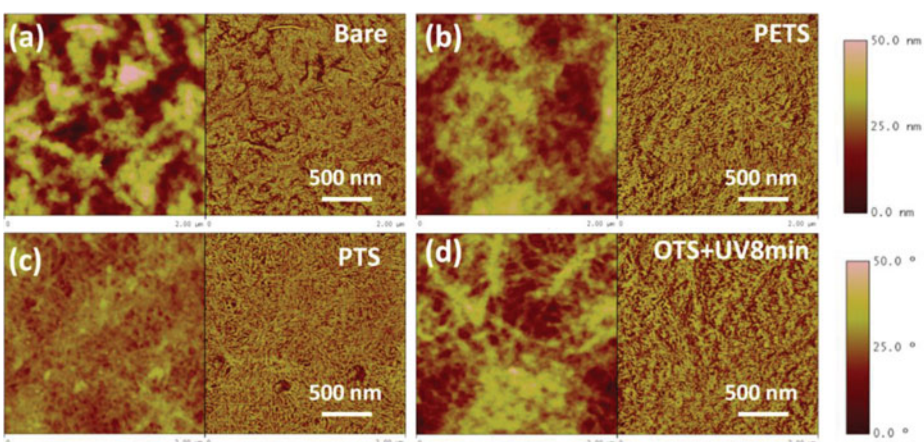

Figure 7. AFM images (2 μm × 2 μm) of the inkjet printed P3HT films on the substrates with different treatments.

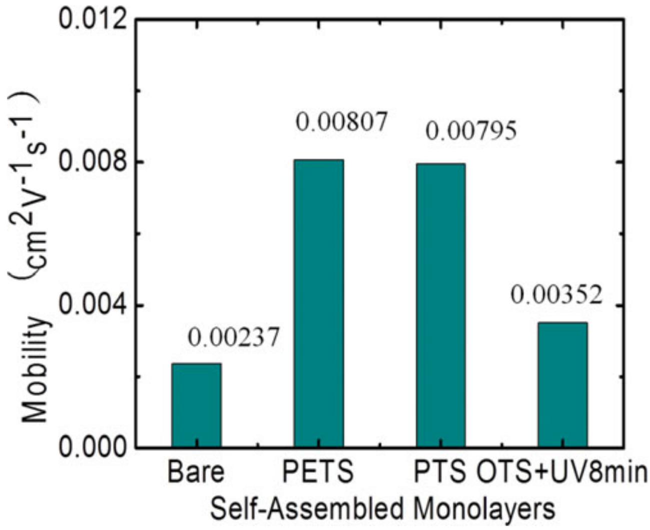

Figure 8. The best field-effect characteristics of the inkjet printed OTFTs with different dielectric surface treatments. ($W = 800\ \mu$m, $L = 80\ \mu$m).

The AFM phase images of the films formed on PETS and PTS treated surface shows well-defined nanometer-scale fibers with a diameter on the order of 30–50 nm and an height on the order of 3–5 nm. These nanofibers are similar to the crystalline structures observed in the P3HT films reported by others [24, 33]. It has been demonstrated that the extended P3HT chains in the nanofibers preferentially packed parallel to each other, with their long-chain axis perpendicular to the length direction of the fiber. The structure enables charge transport in the 2D conjugation direction, i.e., along the axis of the nanofiber, thus contributes to enhanced the charge carrier mobility in the TFT devices. However, the AFM phase images of the P3HT films on bare and OTS + UV8min-treated silicon wafers showed much less ordering feature compared with those on PETS and PTS treated surfaces. The difference in micro-morphology can be ascribed to the different evaporation rate. The diameter of the droplets on the PETS and PTS treated surface were smaller than those on the bare and OTS + UV8min-treated surface. The smaller contact diameter tends to slow down the solvent evaporation and elongate the solidification time. A longer solidification time can facilitate the growth of a highly crystalline film because P3HT chains can self-organize over a long period of time to form thermodynamically favored crystalline structures [34, 35]. Therefore, the films on the PETS and PTS treated surface had better structural ordering.

Fig. 8 shows the field-effect characteristics of the inkjet printed OTFTs on different SAM-treated gate dielectrics. The field-effect mobility of each transistor was calculated in the saturation regime (V_{DS} = –60 V) by plotting the square root of the drain current versus the gate voltage (Fig. 9) and fitting the data to the following equation:

$$I_{DS} = \frac{WC_i}{2L}\mu(V_{GS} - V_T)^2$$

where $C_i = 10.8\ n$F cm^{-2}, $L = 80\ \mu$m, and $W = 800\ \mu$m.

Fig. 9 shows the transport and output curves of the best-performing OTFTs fabricated on the SiO_2 gate dielectrics with different surface treatments. When a bare SiO_2 layer or the OTS + UV8min layer was applied, the best field-effect mobility of inkjet printed

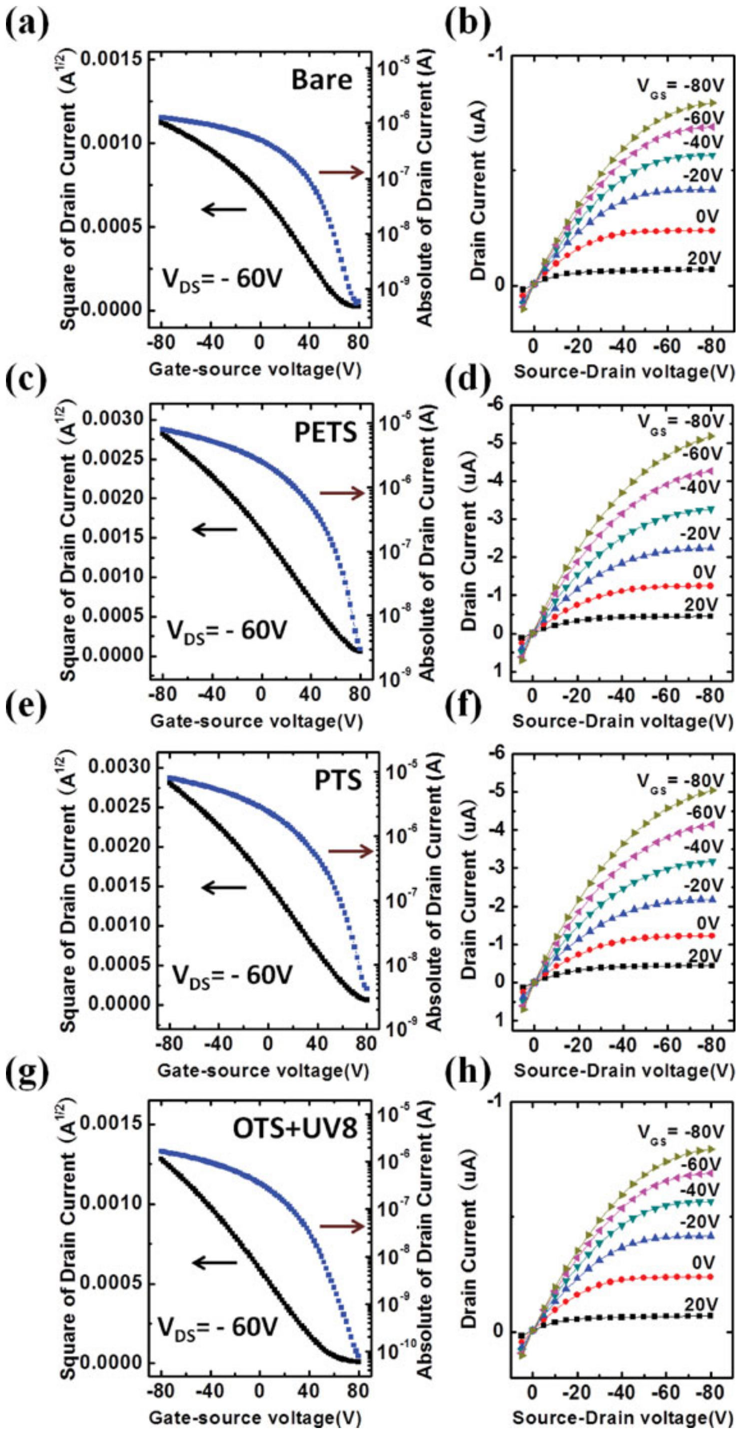

Figure 9. Transfer (a, c, e, and g) and output characteristics (b, d, f, and h) of the inkjet printed OTFTs with different dielectric surface treatments.

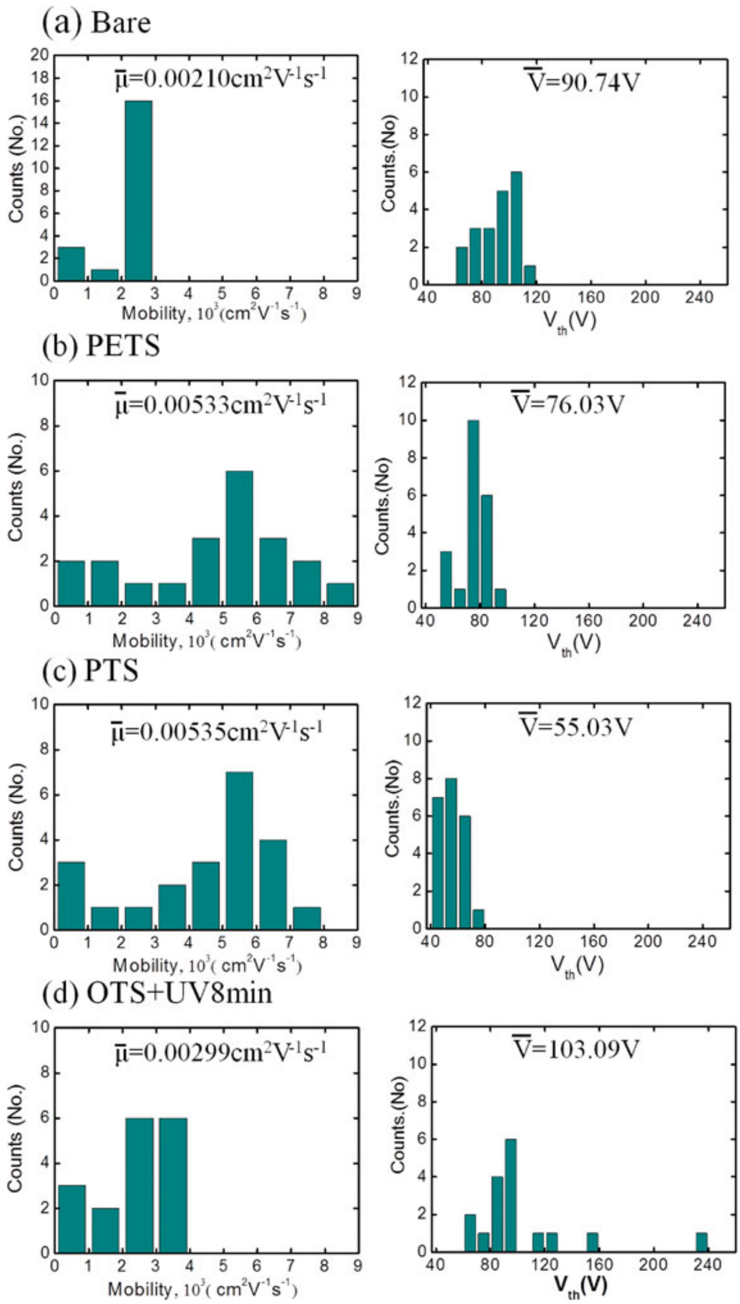

Figure 10. (a, b, c, and d) Summary of the device characteristics for 20, 21, 22, and 17 of 30 inkjet printed transistors with different dielectric surface treatments. The field-effect mobility (μ), and threshold voltage (Vth) were obtained from the transfer curves in the saturation regime ($V_{DS} = -60$ V)

OTFT devices was only 2.37×10^{-3} cm^{2}V^{-1}s^{-1} and 3.52×10^{-3} cm^{2}V^{-1}s^{-1}, respectively. When the PETS treatment or the PTS treatment was applied on the SiO_2 dielectric layer, the field-effect performances were substantially improved and the best field-effect mobility was enhanced to 8.07×10^{-3} cm^{-2}V^{-1}s^{-1} and 7.95×10^{-3} cm^{-2}V^{-1}s^{-1}, respectively, while the on/off current ratios reached 10^3. All inkjet printed P3HT transistors have high threshold voltages. This shift in threshold voltage can be ascribed to the doping of P3HT with oxygen and moisture because the film processing and device measurement were performed in ambient air environment. It is known that the conductivity of P3HT films was found to increase upon a few minutes exposure to air.

To examine the reproducibility of the printed P3HT OTFT devices, the electrical properties of 30 transistors were examined for each treatments. The numbers of devices showed the field-effect characteristics were 20, 21, 22, and 17 on bare, PETS-, PTS-, and OTS + UV8min treated substrates, respectively. Fig. 10 shows that the average field-effect characteristics obtained from the printed P3HT OTFTs on different substrates. It can be clearly observed that the devices with PETS treatment or PTS treatment exhibited the highest field-effect mobility both in the best value and on average. Moreover, the threshold voltage (V_{TH}) was also better than devices without SAM layers. Consequently, it is confirmed that PETS treatment and PTS treatment on the SiO_2 dielectric layer in OTFTs can effectively improved the device performances by contributing to the self-organized formation of P3HT. This phenomenon shows that the surface property not only substantially affected the morphologies of inkjet-printed single droplets and films of P3HT, but also the electrical performance of the inkjet printed OTFT devices. The field-effect mobility was enhanced when the semiconductor is printed on substrates with lower surface energy.

Furthermore, the field-effect characteristic of the OTFT devices was effectively optimized with the different SAM treatments. The self-assemble monolayer of PETS and PTS were found to be the most suitable material for SAM treatment of the substrate for the inkjet printed OTFTs among all the SAMs in this work. It may be explained by the fact that the surface energy of PETS and PTS SAMs are comparable to the surface tension of trichorobezene (i.e., 39.9 dyne/cm), thus the ink droplets wet well on these substrates, which can promote the self-organization of P3HT and form interconnected P3HT fibrils in the inkjet printed films.

Acknowledgments

This work was supported by the National Basic Research Program of China (Grant No. 2012CB723406), the National Natural Science Foundation of China (61040015, 51103034, 21174036, 61107014, and 51203039), the Program for New Century Excellent Talents in University (Grant No. NCET-12-0839), the Research Fund for the Doctoral Program of Higher Education of China (20100111120006).

References

[1] Braga, D., & Horowitz, G. (2009). High-performance organic field-effect transistors. *Adv. Mater.*, *21*, 1473–1486.

[2] Sirringhaus, H., Bird, M., Richards, T., & Zhao, N. (2010). Charge transport physics of conjugated polymer field-effect transistors. *Adv. Mater.*, *22*, 3893–3898.

[3] Tobjork, D., & Osterbacka, R. (2011). Paper electronics. *Adv. Mater.*, *23*, 1935–1961.

[4] Anthony, J. E. (2008). The larger acenes: Versatile organic semiconductors. *Angew. Chem. Int. Ed.*, *47*, 452–483.

[5] Głowacki, E. D., Irimia-Vladu, M., Kaltenbrunner, M., Gsiorowski, J., White, M. S., Monkowius, U., Romanazzi, G., Suranna, G. P., Mastrorilli, P., Sekitani, T., Bauer, S., Someya, T., Torsi, L., & Sariciftci, N. S. (2013). Hydrogen-bonded semiconducting pigments for air-stable field-effect transistors. *Adv. Mater.*, *25*, 1563–1569.

[6] Bao, Z., Dodabalapur, A., & Lovinger, A. J. (1996). Soluble and processable regioregular poly(3-hexylthiophene) for thin film field-effect transistor applications with high mobility. *Appl. Phys. Lett.*, *69*, 4108–4110.

[7] Wang, C. L., Dong, H. L., Hu, W. P., Liu, Y. Q., & Zhu, D. B. (2012). Semiconducting pi-conjugated systems in field-effect transistors: A material odyssey of organic electronics. *Chem. Rev.*, *112*, 2208–2267.

[8] Smith, J., Hamilton, R., McCulloch, I., Stingelin-Stutzmann, N., Heeney, M., Bradley, D. D. C., & Anthopoulos, T. D. (2010). Solution-processed organic transistors based on semiconducting blends. *J. Mater. Chem.*, *20*, 2562–2574.

[9] Rogers, J. A., Bao, Z. N., Makhija, A., & Braun, P. (1999). Printing process suitable for reel-to-reel production of high-performance organic transistors and circuits. *Adv. Mater.*, *11*, 741–745.

[10] Kang, H., Kitsomboonloha, R., Jang, J., & Subramanian, V. (2012). High-performance printed transistors realized using femtoliter gravure-printed sub-10 μm metallic nanoparticle patterns and highly uniform polymer dielectric and semiconductor layers. *Adv. Mater.*, *24*, 3065–3069.

[11] Hwang, J. K., Cho, S., Dang, J. M., Kwak, E. B., Song, K., Moon, J., & Sung, M. M. (2010). Direct nanoprinting by liquid-bridge-mediated nanotransfer moulding. *Nat. Nanotechnol.*, *5*, 742–748.

[12] Hansen, C. J., Saksena, R., Kolesky, D. B., Vericella, J. J., Kranz, S. J., Muldowney, G. P., Christensen, K. T., & Lewis, J. A. (2013). High-throughput printing via microvascular multinozzle arrays. *Adv. Mater.*, *25*, 96–102.

[13] Sirringhaus, H., Kawase, T., Friend, R. H., Shimoda, T., Inbasekaran, M., Wu, W., & Woo, E. P. (2000). High-resolution inkjet printing of all-polymer transistor circuits. *Science*, *290*, 2123–2126.

[14] Sekitani, T., Noguchi, Y., Zschieschang, U., Klauk, H., & Someya, T. (2008). Organic transistors manufactured using inkjet technology with subfemtoliter accuracy. *PNAS*, *105*, 4976–4980.

[15] James, D. T., Kjellander, B. K. C., Smaal, W. T. T., Gelinck, G. H., Combe, C., McCulloch, I., Wilson, R., Burroughes, J. H., Bradley, D. D. C., & Kim, J. S. (2011). Thin-film morphology of inkjet-printed single-droplet organic transistors using polarized raman spectroscopy: Effect of blending TIPS-pentacene with insulating polymer. *Acs Nano*, *5*, 9824–9835.

[16] Singh, M., Haverinen, H. M., Dhagat, P., & Jabbour, G. E. (2010). Inkjet printing-process and its applications. *Adv. Mater.*, *22*, 673–685.

[17] Madec, M. B., Smith, P. J., Malandraki, A., Wang, N., Korvink, J. G., & Yeates, S. G. (2010). Enhanced reproducibility of inkjet printed organic thin film transistors based on solution processable polymer-small molecule blends. *J. Mater. Chem.*, *20*, 9155–9160.

[18] Tseng, H. Y., & Subramanian, V. (2011). All inkjet-printed, fully self-aligned transistors for low-cost circuit applications. *Org. Electron.*, *12*, 249–256.

[19] Arias, A. C., Daniel, J., Sambandan, S., Ng, T. N., Russo, B., Krusor, B., & Street, R. A. (2008). All printed thin film transistors for flexible electronics. *Proceedings of the SPIE - The International Society for Optical Engineering*, 2008, 70540L-70541-70547.

[20] Lim, J. A., Kim, J. H., Qiu, L., Lee, W. H., Lee, H. S., Kwak, D., & Cho, K. (2010). Inkjet-printed single-droplet organic transistors based on semiconductor nanowires embedded in insulating polymers. *Adv. Funct. Mater.*, *20*, 3292–3297.

[21] Chang, P. C., Lee, J., Huang, D., Subramanian, V., Murphy, A. R., & Frechet, J. M. J. (2004). Film morphology and thin film transistor performance of solution-processed oligothiophenes. *Chem. Mater.*, *16*, 4783–4789.

[22] Plotner, M., Wegener, T., Richter, S., Howitz, S., & Fischer, W. J. (2004). Investigation of ink-jet printing of poly-3-octylthiophene for organic field-effect transistors from different solutions. *Synth. Met.*, *147*, 299–303.

[23] Lee, S. H., Choi, M. H., Han, S. H., Choo, D. J., Jang, J., & Kwon, S. K. (2008). High-performance thin-film transistor with 6,13-bis(triisopropylsilylethynyl) pentacene by inkjet printing. *Org. Electron.*, *9*, 721–726.
[24] Kline, R. J., McGehee, M. D., & Toney, M. F. (2006). Highly oriented crystals at the buried interface in polythiophene thin-film transistors. *Nat. Mater.*, *5*, 222–228.
[25] Yoon, M. H., Kim, C., Facchetti, A., & Marks, T. J. (2006). Gate dielectric chemical structure-organic field-effect transistor performance correlations for electron, hole, and ambipolar organic semiconductors. *J. Am. Chem. Soc.*, *128*, 12851–12869.
[26] Majewski, L., & Grell, M. (2005). Organic field-effect transistors with ultrathin modified gate insulator. *Synth. Met.*, *151*, 175–179.
[27] Veres, J., Ogier, S., Lloyd, G., & De Leeuw, D. (2004). Gate insulators in organic field-effect transistors. *Chem. Mater.*, *16*, 4543–4555.
[28] Salleo, A., Chabinyc, M. L., Yang, M. S., & Street, R. A. (2002). Polymer thin-film transistors with chemically modified dielectric interfaces. *Appl. Phys. Lett.*, *81*, 4383–4385.
[29] Kobayashi, S., Nishikawa, T., Takenobu, T., Mori, S., Shimoda, T., Mitani, T., Shimotani, H., Yoshimoto, N., Ogawa, S., & Iwasa, Y. (2004). Control of carrier density by self-assembled monolayers in organic field-effect transistors. *Nat. Mater.*, *3*, 317–322.
[30] Wu, Y. O., Liu, P., Ong, B. S., Srikumar, T., Zhao, N., Botton, G., & Zhu, S. P. (2005). Controlled orientation of liquid-crystalline polythiophene semiconductors for high-performance organic thin-film transistors. *Appl. Phys. Lett.*, *86*.
[31] Wang, X. H., Xiong, X. F., Qiu, L. Z., & Qiang Lv, G. (2012). Morphology of inkjet printed 6, 13 bis (tri-isopropylsilylethynyl) pentacene on surface-treated silica. *Journal of Vacuum Science & Technology B: Microelectronics and Nanometer Structures*, *30*, 021206-021206-021206.
[32] Lim, J. A., Lee, W. H., Kwak, D., & Cho, K. (2009). Evaporation-induced self-organization of inkjet-printed organic semiconductors on surface-modified dielectrics for high-performance organic transistors. *Langmuir*, *25*, 5404–5410.
[33] Yang, H. C., Shin, T. J., Yang, L., Cho, K., Ryu, C. Y., & Bao, Z. N. (2005). Effect of mesoscale crystalline structure on the field-effect mobility of regioregular poly(3-hexyl thiophene) in thin-film transistors. *Adv. Funct. Mater.*, *15*, 671–676.
[34] Chang, J. F., Sun, B. Q., Breiby, D. W., Nielsen, M. M., Solling, T. I., Giles, M., McCulloch, I., & Sirringhaus, H. (2004). Enhanced mobility of poly(3-hexylthiophene) transistors by spin-coating from high-boiling-point solvents. *Chem. Mater.*, *16*, 4772–4776.
[35] Kim, D. H., Jang, Y., Park, Y. D., & Cho, K. (2006). Controlled one-dimensional nanostructures in poly(3-hexylthiophene) thin film for high-performance organic field-effect transistors. *J. Phys. Chem. B*, *110*, 15763–15768.